THE JOURNAL OF BIOLOGICAL CHEMISTRY VOL. 292, NO. 7, pp. 2944–2955, February 17, 2017

Comparing Galactan Biosynthesis in *Mycobacterium tuberculosis* and *Corynebacterium diphtheriae*[*]

Received for publication, September 18, 2016, and in revised form, December 28, 2016 Published, JBC Papers in Press, December 30, 2016, DOI 10.1074/jbc.M116.759340

Darryl A. Wesener[‡1,2], **Matthew R. Levengood**[§1,3], **and Laura L. Kiessling**[‡§4]

From the [‡]*Department of Biochemistry and* [§]*Department of Chemistry, University of Wisconsin-Madison, Madison, Wisconsin 53706*

Edited by Gerald W. Hart

The suborder Corynebacterineae encompasses species like *Corynebacterium glutamicum*, which has been harnessed for industrial production of amino acids, as well as *Corynebacterium diphtheriae* and *Mycobacterium tuberculosis*, which cause devastating human diseases. A distinctive component of the Corynebacterineae cell envelope is the mycolyl-arabinogalactan (mAG) complex. The mAG is composed of lipid mycolic acids, and arabinofuranose (Ara*f*) and galactofuranose (Gal*f*) carbohydrate residues. Elucidating microbe-specific differences in mAG composition could advance biotechnological applications and lead to new antimicrobial targets. To this end, we compare and contrast galactan biosynthesis in *C. diphtheriae* and *M. tuberculosis*. In each species, the galactan is constructed from uridine 5′-diphosphate-α-D-galactofuranose (UDP-Gal*f*), which is generated by the enzyme UDP-galactopyranose mutase (UGM or Glf). UGM and the galactan are essential in *M. tuberculosis,* but their importance in Corynebacterium species was not known. We show that small molecule inhibitors of UGM impede *C. glutamicum* growth, suggesting that the galactan is critical in corynebacteria. Previous cell wall analysis data suggest the galactan polymer is longer in mycobacterial species than corynebacterial species. To explore the source of galactan length variation, a *C. diphtheriae* ortholog of the *M. tuberculosis* carbohydrate polymerase responsible for the bulk of galactan polymerization, GlfT2, was produced, and its catalytic activity was evaluated. The *C. diphtheriae* GlfT2 gave rise to shorter polysaccharides than those obtained with the *M. tuberculosis* GlfT2. These data suggest that GlfT2 alone can influence galactan length. Our results provide tools, both small molecule and genetic, for probing and perturbing the assembly of the Corynebacterineae cell envelope.

[*] This work was supported by National Institutes of Health Grants R01GM055984 and R01AI063596 (to L. L. K). The authors declare that they have no conflicts of interest with the contents of this article. The content is solely the responsibility of the authors and does not necessarily represent the official views of the National Institutes of Health.

[1] Both authors contributed equally to this work.

[2] Recipient of fellowships from the National Science Foundation Graduate Research Fellowship and the National Institutes of Health Chemistry-Biology Interface Training Program Fellowship (T32 GM008505), which is supported the University of Wisconsin-Madison, Office of the Vice Chancellor for Research and Graduate Education with funding from the Wisconsin Alumni Research Foundation, for fellowships.

[3] Supported by a National Institutes of Health Postdoctoral Fellowship (F32GM089219).

[4] To whom correspondence should be addressed: Dept. of Chemistry, University of Wisconsin-Madison, 1101 University Ave., Madison, WI, 53706. Tel.: 608-262-0541; Fax: 608-265-0764; E-mail: kiessling@chem.wisc.edu.

Mycobacterium tuberculosis and *Corynebacterium diphtheriae*, the etiological agents of tuberculosis and diphtheria, respectively, are notorious members of the bacterial suborder Corynebacterineae. This taxon includes other pathogenic bacterial species, including the causative agents of leprosy, nocardiosis, and buruli ulcers. One notable feature of Corynebacterineae is the cell envelope, which has a unique composition. The Corynebacterineae cell envelope contains mycolic acids appended to branched polymers of Ara*f* (arabinan),[5] which are linked to peptidoglycan through a linear polymer of Gal*f* (galactan) (1, 2). The macromolecular structure that extends beyond the peptidoglycan is referred to as the mAG complex. Neither the mAG nor its individual components are present in host mammals. Moreover, in *M. tuberculosis* the mAG complex serves as a barrier to antitubercular drugs and can modulate the human immune response in favor of bacterial immune evasion (3, 4). A complete understanding of mAG assembly and variation could yield novel strategies for therapeutic intervention.

Structural features of the mycobacterial and corynebacterial cell envelopes have been characterized (Fig. 1) (5–11). The galactan is anchored to the peptidoglycan at the C-6 position of peptidoglycan muramic acid. The linker includes a phosphodiester-linked 1-α-D-*N*-acetylglucosamine residue with an α-substituted L-rhamnopyranosyl residue at the 3 position (Fig. 2). The 4-position of rhamnose is substituted with the galactan, a polymer of alternating β(1–5)- and β(1–6)-linked β-D-Gal*f* residues. The enzymes the mediate galactan biosynthesis in mycobacteria have been identified. Two galactofuranosyltransferases, GlfT1 and GlfT2, generate the galactan using UDP-Gal*f*, the activated Gal*f* sugar donor afforded by the action of UGM (12, 13). GlfT1 catalyzes the addition of two to three Gal*f* residues to the C-4 hydroxyl of L-rhamnose (14, 15). The galactofuranosyl polymerase GlfT2 then promotes the sequential addition of the alternating β(1–5) and β(1–6) Gal*f* linkages (16–19). After galactan polymerization, 3 α-Ara*f* residues are added to the C-5 hydroxyl groups of the 8th, 10th, and 12th Gal*f* residues of the galactan (20). Arabinofuranosyltransferases elaborate these residues to append a branched Ara*f* polysaccharide. Subsequently, multiple terminal Ara*f* residues are acylated to form long chain mycolic acid esters. Enzymes involved in mycolic acid biosynthesis or arabinan production are the targets of clinically used antitubercular drugs (21).

[5] The abbreviations used are: Ara*f*, arabinofuranose; FP, fluorescence polarization; Gal*f*, galactofuranose; Gal*p*, galactopyranose; mAG, mycolyl-arabinogalactan; UGM, uridine 5′-diphosphate galactopyranose mutase.

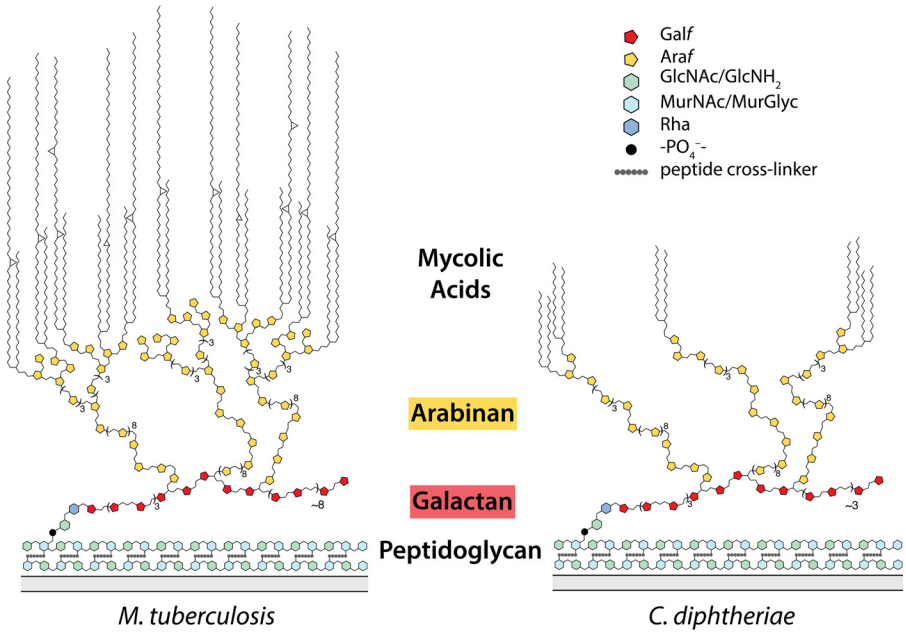

FIGURE 1. **Comparative models of the structure of the mAG complex.** Schematic comparison of the mAG complex from *M. tuberculosis* and *C. diphtheriae* cell walls.

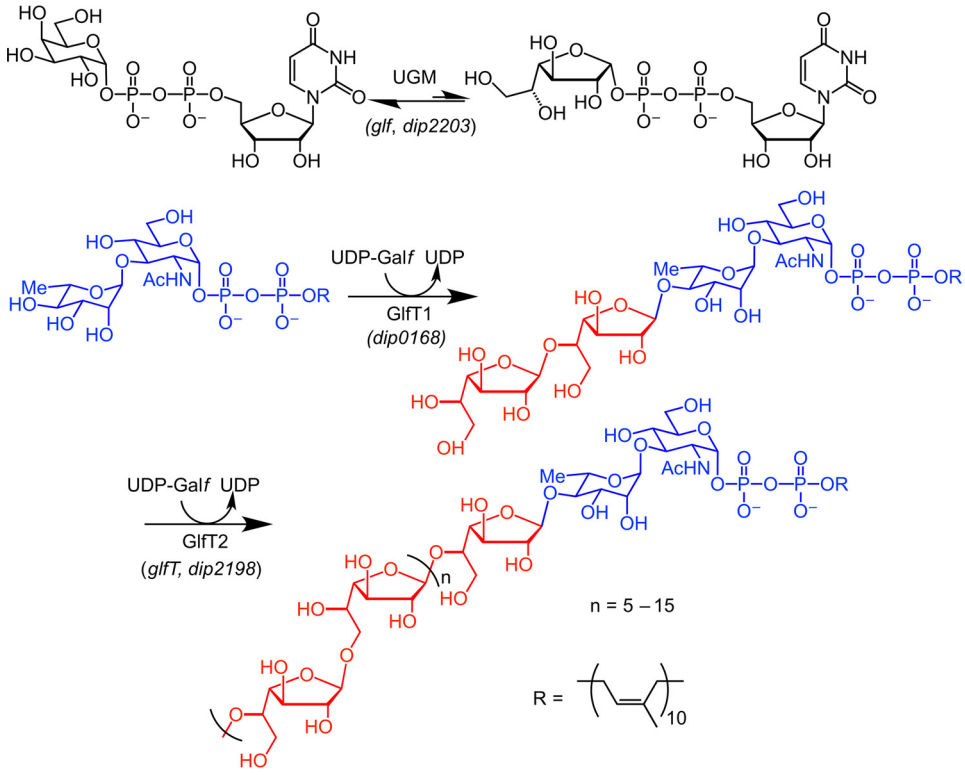

FIGURE 2. **Proposed enzymatic reactions in galactan biosynthesis in *C. diphtheriae*.**

Although mAG biosynthesis and structure is often studied in *M. tuberculosis*, *Corynebacterium* species have recently been used as models to understand mAG assembly. Their advantages include a decreased doubling time, reduced biosafety designation, and the availability of tools for genetic manipulation (22–25). Although most mAG biosynthetic genes are essential in *M. tuberculosis* (26), their deletion in *C. glutamicum* often yields slow growing but viable mutants. For example, *C. glutamicum* mutants lacking AftA were recently used to determine that this arabinofuranoysltransferase appends three α(1–5)–Ara*f* residues to the galactan to initiate arabinan biosynthesis (27). Another *C. glutamicum* mutant revealed Pks13 catalyzes the final step of mycolic acid biosynthesis in corynebacteria and mycobacteria (24). Unexpectedly, a *C. glutamicum* mutant lacking the first enzyme required for activated Ara*f* donor sugar biosynthesis, *ubiA*, is viable (20). This strain is devoid of Ara*f*, and that it could be isolated and cultured was surprising. These examples highlight how experiments using

Corynebacterium species can provide important insight into cell envelope biosynthesis within the Corynebacterineae suborder.

Although each Corynebacterineae species possesses an mAG of similar constitution, fine structural features of the mAG can vary. The arabinan of *C. diphtheriae* lacks the 1,3,5-linked Ara*f* residues that are responsible for branching, suggesting this arabinan is less complex than that of other Corynebacterineae (7). Accordingly, arabinan assembly in mycobacteria is mediated by a larger collection of enzymes. Six or more arabinofuranosyltransferases are involved in mycobacteria, and at least one of these enzymes is inhibited by the first-line antitubercular drug ethambutol (28–30). Of the six mycobacterial arabinofuranosyltransferases, three belong to the Emb family of enzymes. In contrast, corynebacteria encode a single Emb homolog that is most closely related to *M. tuberculosis* EmbC (20). Thus, the arabinan of *C. diphtheriae* is generated using fewer enzymes and is simpler than that of *M. tuberculosis.* The mycolic acids from *Mycobacterium* and *Corynebacterium* species also vary. Mycobacterial mycolic acids possess chains of 70–90 carbon atoms, whereas the mycolic acids of *C. diphtheriae* are shorter, with a chain of 30–36 carbons (7, 31). Additionally, *M. tuberculosis* mycolic acids commonly contain functionalities such as *cis*-cyclopropane that are absent from fast-growing *Mycobacterium smegmatis* or corynebacterial mycolic acids. There also are differences in the galactan. Analyses of the galactan length (20) indicate the corynebacterial galactan is shorter than that of *M. tuberculosis* (5, 7, 27, 32). Understanding the source of these differences can lend insight into the molecular basis for the cell envelope properties of specific species.

The *M. tuberculosis* glycosyltransferase GlfT2 (EC 2.4.1.288) is a bifunctional carbohydrate polymerase that generates the bulk of the galactan (17–19, 33). Studies with chain-terminating glycosyl donors indicate that GlfT2 is sequence-selective, and its fidelity for forming a sequence of alternating β(1–5) and β(1–6) linkages is high (34, 35). Within the GlfT2 polypeptide is but a single active site (33, 36); site-directed mutagenesis indicates substitution of key amino acids abrogates the formation of both β(1–5) and β(1–6) linkages (36). Experiments with isotope-labeled acceptors reveal that GlfT2 is processive (37), and its propensity for generating alternating β(1–5) or β(1–6) Gal*f* linkages is a consequence of processive elongation (38). The enzyme not only controls polymer sequence but also polymer length. In a test tube GlfT2 can generate polymers of a similar length to those obtained from cells (19). With synthetic acceptors, the identity of the anomeric lipid was a critical determinant of product polysaccharide length (17–19). Acceptors with short alkyl anomeric substituents afforded only short oligomeric saccharides, whereas those with longer lipids on the acceptor afforded polysaccharide products similar to those in cells. These findings led to the proposal that *M. tuberculosis* GlfT2 uses the acceptor lipid as a tether and that polymer length is controlled by bivalent substrate binding (19). The D*X*D motif mediates glycosyltransferase coordination to a divalent cation, and *M. tuberculosis* GlfT2 variants in this D*X*D motif afforded truncated oligosaccharide products (36, 39). Thus, GlfT2 is bifunctional with the ability to control the length of polymerized *M. tuberculosis* galactan. Whether these attributes of the *M. tuberculosis* GlfT2 are preserved in other Corynebacterineae species is unclear.

To compare and contrast galactan biosynthesis in different species, we examined the galactan biosynthetic enzymes from *C. glutamicum* and *C. diphtheriae* NCTC 13129, including GlfT2 and UGM. The putative *C. diphtheriae* UGM (DIP2203) catalyzes the isomerization of UDP-Gal*p* and UDP-Gal*f* with an efficiency similar to other prokaryotic orthologs. This finding suggests that differences in galactan length are unlikely to arise from differences in cellular concentration of UDP-Gal*f*. To explore the role of the galactan in cells, we employed small molecule UGM inhibitors. These compounds inhibit *C. diphtheriae* UGM *in vitro* and prevent the growth of *C. glutamicum*. These observations support an essential role for the galactan in corynebacteria as well as mycobacteria and suggest that the small molecule UGM inhibitors can be used to probe the cellular roles of Gal*f*. With regard to GlfT2, our results indicate that the DIP2198 gene product is a bifunctional galactofuranosyltransferase similar to the *M. tuberculosis* GlfT2. The corynebacterial glycosyltransferase can elongate synthetic acceptors to afford polysaccharides commensurate in length to those isolated from corynebacteria. As with the *M. tuberculosis* GlfT2, the product polysaccharides attained from variants with amino acid changes in the proposed donor binding site are truncated. These findings indicate that GlfT2 orthologs have an intrinsic ability to control polysaccharide length. This length control mechanism differs from that employed in O-antigen biosynthesis in which length is controlled by an auxiliary protein (40–42). Our investigations lay a foundation for dissecting the molecular details and mechanisms of galactan biosynthesis using genetic and chemical genetic tools.

Results

Inhibitors of Galactan Biosynthesis Block Corynebacterial Growth—Unlike mycobacteria, corynebacteria do not require mycolic acids (24) or arabinan (20). The survival of corynebacteria without integral mAG components raises the issue of whether these species require the galactan. Small molecule UGM inhibitors provide the means to address this issue (Fig. 2) (43). We previously produced the *C. diphtheriae* UGM (DIP2203) (44). In this study we characterized the enzyme's catalytic properties and then identified a *C. diphtheriae* UGM inhibitor that could be used to probe the role of the galactan. The initial velocities of UDP-Gal*p* production were calculated from reaction mixtures containing a range of UDP-Gal*f* concentrations (45, 46). Steady-state kinetic parameters were determined from the Michaelis-Menten equation, which afforded a K_m of 47 $\pm$ 5 μM and a k_{cat} value of 20 $\pm$ 0.6 s^{-1} (Table 1). The enzymatic efficiency, or k_{cat}/K_m, for *C. diphtheriae* UGM is 4.3 $\pm$ 0.5 $\times$ 10^5 $M^{-1}s^{-1}$. These kinetic constants are similar to those obtained with UGM orthologs from other prokaryotes, including those from *Klebsiella pneumoniae* and *Escherichia coli* (46, 47).

Our previous experience suggested that inhibitors of *M. tuberculosis* UGM should act against *C. diphtheriae* UGM (44). To assess compound affinity for UGM, we validated that a previously described fluorescence polarization (FP) assay (48) could be applied to the *C. diphtheriae* UGM. The enzyme

TABLE 1
Michaelis-Menten steady state kinetic parameters of prokaryotic UGM proteins
All activities were measured using UDP-Gal*f* as the substrate in the presence of sodium dithionite

Species	K_m	k_{cat}	$k_{cat/m}$
	μM	s^{-1}	$10^5\ M^{-1}s^{-1}$
C. diphtheriae	47 ± 5	20 ± 0.6	4.3 ± 0.5
K. pneumoniae[a]	43 ± 6	5.5 ± 0.7	1.3 ± 0.2
E. coli[b]	27	22	8.1

[a] From Ref. 47.
[b] From Ref. 46.

bound the fluorescein-bearing UDP derivative with an apparent affinity of 24 ± 2 nM. Small molecules could then be tested for their ability to displace the fluorescent probe from the enzyme in a competition assay (49). Only compounds **1** and **2** were effective. Their calculated dissociation constants were similar, 8 ± 1 μM for **1** and 10 ± 2 μM for **2**. We next evaluated the UGM ligands as inhibitors. As expected from the FP assay results, UDP and compound **3** did not substantially inhibit *C. diphtheriae* UGM activity at 15 μM, but compounds **1** and **2** impeded conversion of UDP-Gal*f* to UDP-Gal*p* by 83 ± 2% and 69 ± 3%, respectively (Fig. 3*B*). At 50 μM UDP-Gal*f*, a concentration near the K_m value we report here, the IC_{50} value of compound **1** was determined to be 5 ± 1 μM.

We tested whether inhibitor **1** could be used ascertain the consequences of inhibiting galactan biosynthesis. *C. glutamicum* (ATCC 13032) is a non-virulent genetically tractable model organism that had been employed to conclude that corynebacteria can survive without mycolic acids or arabinan (20, 24). We anticipated the UGM inhibitor would be effective because the sequence similarity of the *C. diphtheriae* and *C. glutamicum* UGM is 85%. Indeed, exposure of *C. glutamicum* to compound **1** led to growth inhibition (Fig. 3*C*). The results of this chemical genetics experiment suggest that the galactan is the outermost polysaccharide required for corynebacterial growth.

Galactan Polymerization by C. diphtheriae—The *C. diphtheriae* GlfT2 (DIP2198 gene) and *M. tuberculosis* GlfT2 share 57% amino acid identity, but cell wall analysis indicates that the length of the galactan in corynebacteria is shorter than that in *M. tuberculosis.* This difference prompted us to compare the catalytic properties of the GlfT2 orthologs. If GlfT2 can control galactan length, the *C. diphtheriae* enzyme should give rise to shorter polymers than those afforded by *M. tuberculosis* GlfT2. We produced a His-tagged *C. diphtheriae* GlfT2 and monitored its carbohydrate polymerase activity using matrix-assisted laser desorption/ionization (MALDI) mass spectrometry (19, 37). The reaction conditions employed with acceptor **4a** (Fig. 4) were similar to those used to assay *M. tuberculosis* GlfT2 activity. Polysaccharides were attained demonstrating that the DIP2198 gene product can generate polymers of galactofuranose (Fig. 4*B*, *left*). On the basis of previous studies with *M. tuberculosis* GlfT2 (17, 18, 33, 36), we anticipated that the *C. diphtheriae* GlfT2 product polysaccharides would be composed of alternating $\beta(1-6)$– and $\beta(1-5)$–Gal*f* linkages. We, therefore, also examined elongation from disaccharide acceptor, compound **5,** which has a $\beta(1-5)$–Gal*f* linkage and, therefore, is a regioisomer of acceptor **4a** (36). The *C. diphtheriae* GlfT2 also elongated compound **5** to afford polymers of similar length to those attained with **4a** (Fig. 4*B*, *right*). The ability of both synthetic acceptors to function as substrates of *C. diphtheriae* GlfT2 suggests the enzyme catalyzes formation of both $\beta(1-6)$– and $\beta(1-5)$–Gal*f* glycosidic linkages.

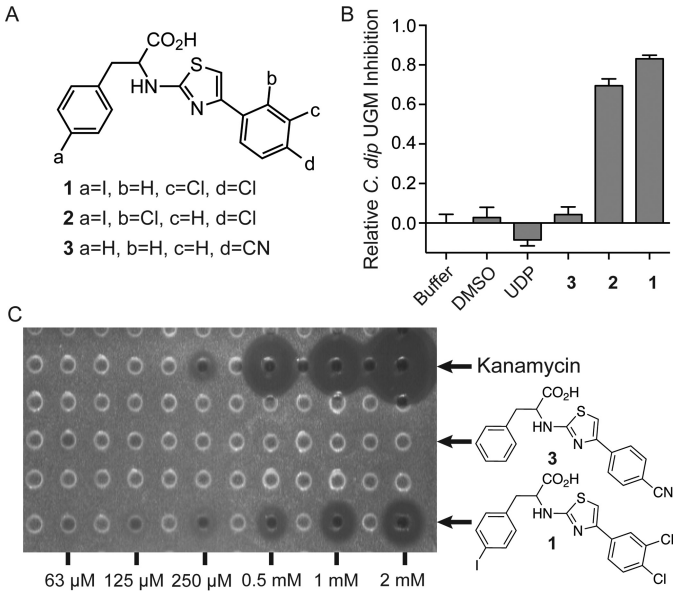

FIGURE 3. **Chemical inhibition of *C. glutamicum* growth.** *A*, chemical structure of 2-aminothiazole small molecule UGM inhibitors employed in this study. *B*, *in vitro* inhibition of *C. diphtheriae* UGM activity by the small molecules (15 μM) shown in *A*. Compound **3** has the same chemotype as compounds **1** and **2** yet fails to inhibit *C. diphtheriae* UGM. Data are shown as the mean ± S.D. ($n = 3$ technical replicates). *C*, inhibition of *C. glutamicum* growth by UGM inhibitor **1.** The antibiotic kanamycin was used as a known inhibitor of cell growth. DMSO treatment was used as a vehicle control, and samples treated with compound **3** were tested as a chemotype control. The concentration of a 10-μl solution of **1** added to each well is included below the image. The result is representative of three biological replicates.

Both the *M. tuberculosis* and *C. diphtheriae* GlfT2 enzymes generate Gal*f* polymers, but mass spectrometry analysis suggested that the polymeric products from the *C. diphtheriae* ortholog are substantially shorter than those from *M. tuberculosis* GlfT2 (Fig. 4*C*). We, therefore, examined the rate of polymerization by *C. diphtheriae* GlfT2. We employed compound **4a** in a coupled continuous enzyme assay that monitors the release of UDP (50). The data indicate that *C. diphtheriae* GlfT2 is a slower polymerase than is *M. tuberculosis* GlfT2. Under the same conditions (1.25 mM UDP-Gal*f* and 0.2 mM **4a**), the *C. diphtheriae* GlfT2 was ~17-fold slower than the *M. tuberculosis* GlfT2 (0.47 ± 0.24 μM/min for *C. diphtheriae* GlfT2 *versus* 8.2 μM/min for *M. tuberculosis* GlfT2). The slower rate of the *C. diphtheriae* enzyme was not a function of decreased protein stability as the *C. diphtheriae* GlfT2 was less prone to aggregation and precipitation than *M. tuberculosis* GlfT2.

Anomeric Lipid Influences Polysaccharide Length—We found previously that the products of the *M. tuberculosis* GlfT2 depend on the attributes of the anomeric lipid of the acceptor. With longer lipid substituents, longer polysaccharide products were obtained (19). We tested whether the *C. diphtheriae* ortholog affords similar results. We used compounds **4b** and **4c** as substrates; the former has a shorter lipid group than our benchmark substrate **4a**, and the latter has a longer lipid substituent. When **4b** was incubated with *C. diphtheriae* GlfT2, no

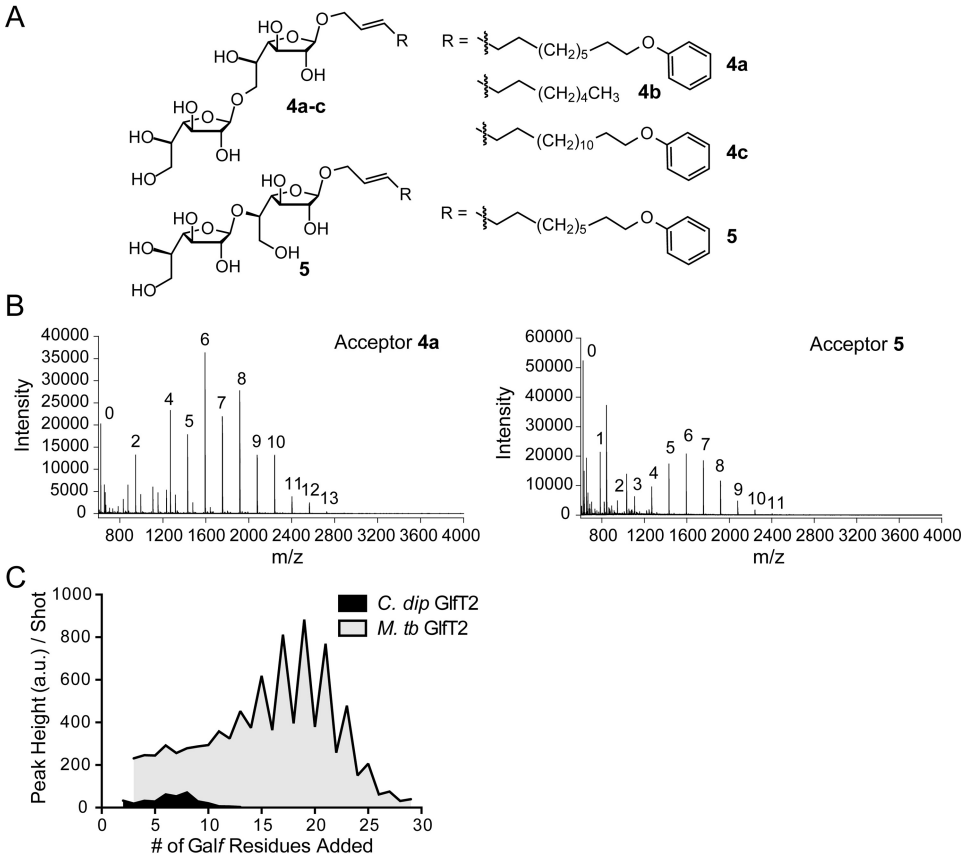

FIGURE 4. **Assessing the polymerase activity of *C. diphtheriae* GlfT2.** *A*, chemical structures of the synthetic acceptors used in this study. *B*, *left*, polymerase activity of *C. diphtheriae* GlfT2 with synthetic acceptor **4a**. *Right*, activity of *C. diphtheriae* GlfT2 using a $\beta(1–5)$ linked disaccharide acceptor substrate, compound **5**. Polymer lengths from *C. diphtheriae* GlfT2 are similar whether the initial disaccharide is $\beta(1–5)$- or $\beta(1–6)$-linked. *C*, comparison of the *in vitro* polymerase activity of *C. diphtheriae* (*C. dip*) GlfT2 and *M. tuberculosis* (*M. tb*) GlfT2. Spectra from the reaction of **4a** with either *M. tuberculosis* GlfT2 or *C. diphtheriae* GlfT2 (Fig. 4*B*, *left*) were overlaid. Spectra were attained from reactions conducted under identical conditions. Product mixtures were analyzed sequentially using MALDI mass spectrometry. From the raw data spectrum, the maximum intensity of each peak is divided by the total number of laser shots used to obtain that spectrum. Results are representative of at least two replicate reactions.

polymeric products were observed (Fig. 5*A*). In contrast, GlfT2-catalyzed elongation of **4c**, a substrate with an extended lipid group, yielded polysaccharide products nearly twice as long, +24 Gal*f* residues (Fig. 5*B*).

Acceptor Glycan Influences Polysaccharide Length—We previously observed a kinetic lag phase for *M. tuberculosis* GlfT2-catalyzed elongation of disaccharide acceptors (37). This lag phase was not observed with trisaccharide or tetrasaccharide acceptors (37, 38). To test *C. diphtheriae* GlfT2 processing of acceptors that vary in the number of saccharide residues, we used a chemoenzymatic approach to generate oligogalactofuranoside acceptors (37). The tetrasaccharide acceptor gave rise to polymeric products up to +32 Gal*f* residues (Fig. 5*C*). These results are consistent with findings that the catalytic site of GlfT2 can accommodate multiple saccharide residues (37). Although the tetrasaccharide afforded substantially longer polymeric products, they remain ~10 residues shorter than those obtained using the *M. tuberculosis* GlfT2 enzyme (38). The rate of *C. diphtheriae* GlfT2-catalyzed polymerization of the tetrasaccharide acceptor is still significantly slower than that obtained with the *M. tuberculosis* enzyme (1.8 μM/min).

Site-directed Mutagenesis for Manipulating Polysaccharide Length—The longer polysaccharide products obtained from the *M. tuberculosis* GlfT2 *versus* the *C. diphtheriae* ortholog suggests that polysaccharide length can be programmed genetically. We previously identified active site residues in the *M. tuberculosis* GlfT2 important for polymerization, and mutant proteins with substitutions in the putative UDP-Gal*f* binding site led to polysaccharides of attenuated length (36). We tested the generality of the mode of length control by installing point mutations at these sites in the *C. diphtheriae* GlfT2. From a primary sequence alignment, we identified two D*X*D motifs within *C. diphtheriae* GlfT2 similar to those found in *M. tuberculosis* GlfT2 (36, 39). By analogy, a DDD motif (residues Asp-273–Asp-275 of *C. diphtheriae* GlfT2) should mediate cation coordination and binding to UDP-Gal*f*, whereas the DDAE motif (Asp-396–Glu-399) should contain the catalytic base (Fig. 6*A*). Accordingly, both *C. diphtheriae* Asp→Ala and Asp→Glu variants were generated at residues Asp-396 and Asp-397. When tested with acceptor **4a**, no elongated products were detected. This abrogation of activity is similar to what was found previously for *M. tuberculosis* GlfT2 (36). The results presented here as well as autoradiographic enzymatic assays and a recent X-ray crystal structure of *M. tuberculosis* GlfT2 (39) all are consistent with the assignment of Asp-397 as the catalytic base in *C. diphtheriae* GlfT2.

We also evaluated GlfT2 variants expected to have altered binding to the glycosyl donor UDP-Gal*f*. A series of Asp→Ala

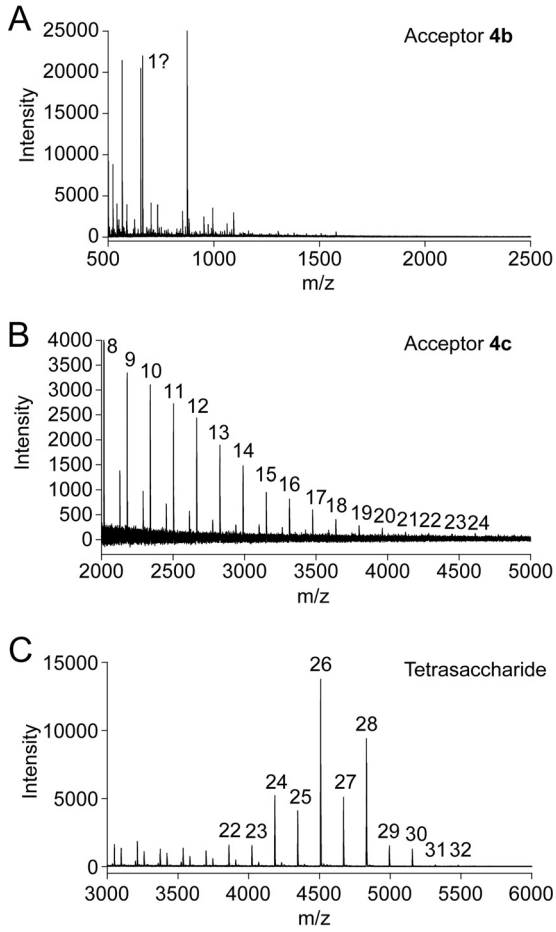

FIGURE 5. **Polysaccharide product profiles attained using *C. diphtheriae* GlfT2.** *In vitro* polymerase activity of *C. diphtheriae* GlfT2 using different acceptors. *A*, MALDI mass spectrum obtained from analysis of the reaction of *C. diphtheriae* GlfT2 with **4b,** a compound with a shorter lipid substituent than **4a.** *B*, MALDI mass spectrum obtained from analysis of the reaction of *C. diphtheriae* GlfT2 with **4c,** a compound with a longer lipid substituent than **4a.** *C*, MALDI mass spectrum resulting from analysis of the reaction of GlfT2 with a tetrasaccharide acceptor generated chemoenzymatically from compound **4a**. Results are representative of at least two replicate reactions.

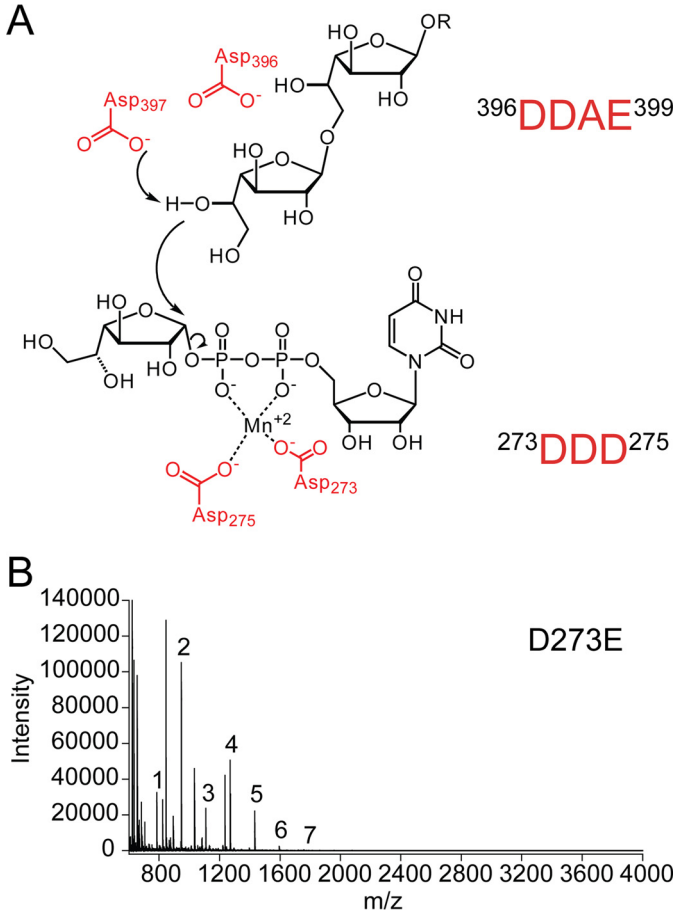

FIGURE 6. **Genetic modulation of *C. diphtheriae* GlfT2 polymerase length control.** *A*, proposed active site structure of *C. diphtheriae* GlfT2 based on mutagenesis results and bioinformatic analysis. *B*, a single Asp→Glu mutation in the glycosyl donor binding site of *C. diphtheriae* GlfT2 yields polymers roughly half the length of wild-type polymer products when using compound **4a** as the acceptor. The tetrasaccharide used is derived from elongation of **4a** by two Gal*f* residues. The result is representative of two replicate reactions.

and Asp→Glu protein substitutions at Asp-273 and Asp-275 were generated. The alanine variants failed to act on compound **4a**. These data contrast with our findings with *M. tuberculosis* GlfT2, as substitution of either aspartic acid residue with an alanine afforded a mutant enzyme that yielded polymeric products (36). Because alanine mutations in the glycosyl donor binding site of *C. diphtheriae* GlfT2 abrogated polymerase activity, we assayed more conservative Asp→Glu variants. In the reaction mixture with the D273E GlfT2, shorter polymeric products were obtained. The longest oligosaccharide detected in the reaction mixture was +6 Gal*f* residues, as compared with +11 Gal*f* using the wild-type protein (Fig. 6*B*). The D273E variant similarly processed the tetrasaccharide acceptor to afford shorter oligosaccharide products. With the D275E variant, no products were detected with either compound **4a** or tetrasaccharide acceptor. As was observed with the *M. tuberculosis* GlfT2, *C. diphtheriae* GlfT2 variants with perturbations in the glycosyl donor binding site afford substantially shorter carbohydrate polymers; the products bore roughly half the number of Gal*f* residues as those produced by wild-type enzyme. These products are unlikely to be substrates for arabinofuranosyltransferases, as arabinan linkage is predicted to occur at Gal*f* residues 8, 10, and 12 within the galactan.

Discussion

The taxon Corynebacterineae includes many bacterial species of industrial and medical importance (51–53). Although Corynebacterineae share cell envelope features, different species occupy distinct ecological niches, and the details of their cell wall composition can vary. Survival in specific physiological environments may have been responsible for alterations in the constitution of their cell envelopes and mAG complexes. The few studies characterizing the mAG of Corynebacterineae species have uncovered structural differences (5, 7, 20, 54). We probed galactan biosynthesis in corynebacteria to better understand the mechanisms by which different species assemble this fundamental component of the mAG complex. We also examined the physiological importance of the mAG using a chemical genetic approach.

Whether disruption of galactan biosynthesis would inhibit corynebacterial growth was an open question as previous experiments have revealed that components once thought to be

essential for Corynebacterineae are dispensable in *C. glutamicum*. Specifically, microbial genetics and chromosomal deletion experiments have shown that mycolic acids (24, 55) and the arabinan are not necessary for viability in this species (20, 27). In contrast, attempts to isolate *M. tuberculosis* mutants with similar genotypes have failed (26). Indeed, no *M. tuberculosis* strains lacking the enzymes that mediate galactan biosynthesis have been isolated, suggesting the galactan is required for *M. tuberculosis* viability.

To test whether the galactan is essential for corynebacterial growth, we used a chemical biology strategy. We determined the catalytic activity of the putative *C. diphtheriae* UGM, DIP2203. This enzyme catalyzes the isomerization of UDP-Gal*p* and UDP-Gal*f* with kinetic parameters similar to those of other prokaryotic UGMs (56–58), and the *C. diphtheriae* enzyme can be inhibited by small molecules developed against the *M. tuberculosis* UGM (43, 44). When our most potent small molecule inhibitor of corynebacteria UGM, compound **1**, was added to *C. glutamicum,* corynebacterial growth was inhibited. This result suggests the galactan is essential in *C. glutamicum*. This finding implies that the peptidoglycan-galactan conjugate is the minimal cell envelope structure needed for viability of corynebacteria, whereas the polysaccharide emanating from the galactan, the arabinan (20), and the cell surface mycolic acids appear dispensable (24).

Previous cell wall analyses suggest that galactose is present at lower abundance in corynebacteria as compared with mycobacteria. This observation suggests that corynebacteria have a shorter galactan (5, 7, 27, 32). The *in vitro* carbohydrate polymerase activity of *C. diphtheriae* GlfT2 gives rise to shorter polymers, consistent with those observations (19). These results indicate that the GlfT2 glycosyltransferases have an intrinsic ability to control length. Our data further suggest that galactan length can be manipulated through mutation or heterologous expression of polymerases. Thus, polysaccharide length is dictated by the enzyme's sequence.

Several other microbial cell envelope glycopolymers possess defined length distributions. These include peptidoglycan, lipopolysaccharide (LPS) O-antigens, capsular polysaccharides, and teichoic acids (59–63). Efforts to elucidate how the length of these polysaccharides is controlled have revealed the importance of accessory proteins. For example, in Wzy-dependent LPS O-antigen biosynthesis product length is controlled by the polysaccharide co-polymerase protein, termed Wzz (40, 61, 64, 65). An *in vitro* polymerization system was used to demonstrate that Wzy alone is sufficient for polymerization, but that addition of Wzz to the reaction can modulate the product length distribution (41). An LPS O-antigen assembled in an ABC transporter-dependent manner also employs an independent chain-length regulator protein. In *E. coli* serotype O9a O-antigen assembly, an extended coiled-coil in the chain length regulator WbdD operates as a molecular ruler to physically separate the kinase termination activity of WbdD, from the glycosylpolymerase activity of WbdA (42). Unlike these systems, there are no apparent accessory proteins that can modulate the length of polysaccharides generated by GlfT2. The galactan and LPS O-antigen are dissimilar in that the galactan is an essential component of the cell envelope, whereas O-antigen is not required for survival and likely evolved for host interactions (66). Bacteria may have evolved unique accessory proteins to alter O-antigen length as a mechanism for modulating surface antigenicity, but such a selective pressure would not be present for galactan assembly.

The mechanisms underlying length control by GlfT2 are unknown. One possibility for the shortened polysaccharide length obtained with *C. diphtheriae* GlfT2 *versus* the *M. tuberculosis* ortholog is that the rate of polymerization for the former is 17-fold slower. Still, the kinetic rate alone is unlikely to be solely responsible for the divergent polymer length distributions we observed. Specifically, the tetrasaccharide acceptor gave rise to longer polysaccharides (+32 Gal*f* residues; Fig. 5*C*) yet the initial velocities observed for *C. diphtheriae* GlfT2 remained slower (1.8 μM/min) than those obtained for *M. tuberculosis* enzyme (8.2 μM/min). Acceptor concentration had little effect on polysaccharide length. When the reaction was conducted at an 8-fold lower acceptor concentration (25 μM compound **4a**), the longest polymer was +15 Gal*f* residues, and a nearly identical product profile was attained. The available data indicate that the features of the acceptor and sequence of the glycosyltransferase modulate product polysaccharide length (19). For example, the longer polymers obtained from the tetrasaccharide *versus* those generated from disaccharide **4a** may be due to the former binding more efficiently and remaining bound through a larger number of catalytic events. Similarly, the affinity of the glycosyl donor may influence polysaccharide product length control. These two catalytic parameters may contribute to GlfT2 length control. Moreover, the data suggest that length of polysaccharides generated by GlfT2 can be modulated through simple mutagenesis. A similar mutagenesis strategy may be useful for modulating the length of other biologically important polysaccharides. Specifically, both GlfT2 and cellulose synthase belong to the glycosyltransferase family 2 (GT-2) glycosylpolymerases (67), and attenuation of cellulose polymer length may be useful for the industrial production of cellulosic derived commodities such as ethanol (68).

A mechanism for carbohydrate polymerase length control based on sugar donor binding has been suggested in an unrelated process; that is, the synthesis of *Streptococcus pneumoniae* type 3 capsular polysaccharide (69). This polysaccharide is generated by a processive synthase. The enzyme uses two sugar donors, UDP-glucose and UDP-glucuronic acid, for [4)-D-Glc-β(1–3)-d-GlcUA-β(1-] polymer formation. Data suggest that the substrate concentrations and the affinity of UDP-glucuronic acid binding to the enzyme influence the product polysaccharide length (69, 70).

The ability of GlfT2 to control polysaccharide length also could rest in an alternative motif. For example, a chain length regulatory proline motif (WPQ) was recently identified in transmembrane glycosyltransferase type 3 arabinofuranosyltransferases (23, 71). Lastly, an alternative hypothesis based on GlfT2 quaternary structure has been put forth (39). The tetrameric structure observed in the *M. tuberculosis* GlfT2 crystals contained a face of mostly hydrophobic and positively charged residues that the authors suggest promotes membrane association. At the center of the tetramer resides a large hollow cavity

TABLE 2
Primers used to generate mutant *glfT2* genes

D273A	5′-GCCTTACATCCTGTACATGGCTGACGACATCGCCATCGAGCCGG-′
D273E	5′-GCCTTACATCCTGTACATGGAAGACGACATCGCCATCGAGCCGG-′
D275A	5′-GCCTTACATCCTGTACATGGATGACGCCATCGCCATCGAGCCGG-′
D275E	5′-GCCTTACATCCTGTACATGGATGACGAAATCGCCATCGAGCCGG-′
D396A	5′-GCCACTGTTTATCAAGTGGGCCGATGCCGAATACGGCTTGCGCG-′
D396E	5′-GCCACTGTTTATCAAGTGGGAAGATGCCGAATACGGCTTGCGCG-′
D397A	5′-GCCACTGTTTATCAAGTGGGACGCTGCCGAATACGGCTTGCGCG-′
D397E	5′-GCCACTGTTTATCAAGTGGGACGAAGCCGAATACGGCTTGCGCG-′

that the authors suggest functions as an area for growing galactan to be displaced into during polymerization, with the size of the cavity influencing product polymer length (39).

Several of the aforementioned mechanisms may contribute to regulating galactan length. For example, the cell membrane may function in a similar role as that proposed for the GlfT2 acceptor anomeric lipid. Thus, the distance between the GlfT2 active site and membrane combined with enzyme binding to substrate would influence the length of polymeric products. We anticipate that future experiments will provide additional insight into how galactan length is controlled.

Experimental Procedures

Synthesis of Substrates, Inhibitors, and Fluorescence Polarization Probe—UDP-Gal*f* was prepared as previously reported (72), as were compounds **1**, **2**, and **3** (43). Acceptor disaccharides **4a-c** and **5** were synthesized using published procedures (19). The FP probe UDP-10C-fluorescein was synthesized as previously described (48). A tetrasaccharide acceptor for GlfT2 derived from compound **4a** was generated by chemoenzymatic synthesis, purified, and characterized as previously described (37).

Cloning of Genes Involved in Galactan Biosynthesis in C. diphtheriae—DIP2198 (*glfT2*) and DIP2203 (*glf*) were cloned from *C. diphtheriae* NCTC 13129 genomic DNA (American Type Culture Collection (ATCC)). The DIP2198 gene (*glfT2*) was amplified via the polymerase chain reaction using the forward primer 5′-GGGAATTC*CATATG*CTTACCATGAGTAAAGCAGTCGAATCACTGC-3′ and the reverse primer 5′-CG*CGGATCCC*TAGGACTCCTCAGCCCCTTGTGGC-3′. The forward and reverse primers added an NdeI and BamHI restriction site, respectively. The purified PCR product and pET-28a(+) vector (EMD Chemicals) were digested with NdeI and BamHI restriction endonucleases (New England Biolabs). The double-digested products were purified using the QIAquick Gel Extraction kit (Qiagen). Digested pET-28a(+) vector and *glfT2* insert were ligated with T4 DNA ligase (Fermentas). The vector encoded N-terminal hexahistidine tag and in-frame insertion of *glfT2* were confirmed by DNA sequence analysis at the UW-Madison Biotechnology Center.

The DIP2203 (*glf*) gene was amplified via the polymerase chain reaction using the forward primer 5′-GGGAATTC-*CATATG*TTGTGGTGCCTAACCCCCATAAGG-3′ and the reverse primer 5′-ATAGTTTA*GCGGCCGC*TTTCAGGGCGTCGACAAGC-3′. The forward and reverse primers added NdeI and NotI restriction sites to the amplicon, respectively. Purified PCR product and pET-24a(+) vector (EMD Chemicals) were digested with NdeI and NotI restriction endonucleases (New England Biolabs). The double-digested products were purified using the QIAquick Gel Extraction kit (Qiagen). Digested pET-24a(+) vector and *glf* insert were ligated with T4 DNA ligase (Fermentas). The vector encoded C-terminal hexahistidine tag, and in-frame insertion of *glf* was confirmed by DNA sequence analysis.

C. diphtheriae GlfT2 Mutagenesis—Sequence analysis was used to identify putative active site resides in *C. diphtheriae* GlfT2. QuikChange mutagenesis (Stratagene) was used to generate point mutations in putative active site residues of the *glfT2* gene. The primer and its reverse complement used to generate *glfT2* mutants are described in Table 2. The underlined triplet codon denotes the mutated residue. The pET-28a::His_6-*glfT2* construct generated in this study was used as the template for the polymerase chain reaction. Template DNA was digested with DpnI (Promega) after PCR amplification. The DpnI-digested mixture was transformed into DH5a *E. coli* by electroporation. Plasmid DNA was isolated using the QIAprep Spin Miniprep kit (Qiagen). Mutation of the desired codon was confirmed by DNA sequence analysis.

Expression of C. diphtheriae glfT2—The gene encoding *C. diphtheriae* His_6-glfT2 was overexpressed and purified using a protocol similar to that employed for *M. tuberculosis* His_6-glfT2 (37). Briefly, a pET-28a plasmid encoding His_6-glfT2 was transformed into BL21(DE3) Tuner *E. coli* cells (Novagen) via electroporation. Cultures from a single colony were grown in Luria-Bertani (LB) medium supplemented with 50 μg/ml kanamycin at 37 °C until A_{600} = 0.8. At this time cultures were placed on ice for 1 h. Protein overexpression was induced by the addition of isopropyl-β-D-thiogalactopyranoside to 0.3 mM. Cultures were allowed to grow at 18 °C for 18–20 h, at which time cells were harvested by centrifugation (5000 × *g*), collected, and stored at −80 °C until use. Cell pellets were thawed on ice in a lysis buffer (20 ml/liter of growth) that contained 50 mM potassium phosphate (pH 7.9), 300 mM sodium chloride (NaCl), 20 mM imidazole, 1:200 protease inhibitor mixture III (Calbiochem) and lysozyme. Cells were disrupted by sonication (Branson Sonifer 450, 5 × 10 s cycles at 90% duty cycle). Lysates were cleared by centrifugation for 1 h at 22,000 × *g*. The soluble lysate was filtered (0.22 mM, Amicon) before loading onto a pre-equilibrated (in lysis buffer) 5-ml HisTrap column (GE Healthcare) at 1.0 ml/min using an AKTA FPLC system (Amersham Biosciences). Protein was eluted using a step gradient of imidazole. Glycerol was added (10% v/v) to 1-ml fractions of >90% purity, with purity assessed by sodium dodecyl sulfate-polyacrylamide gel electrophoresis (SDS-PAGE) and staining with Coomassie Blue. Samples were vitrified in liquid nitrogen and stored at −80 °C until use. Typical yields were 2 mg/liter culture. When performing enzyme assays, a sample of His_6-GlfT2 was removed and dialyzed twice against 2 liters of 50 mM HEPES (pH

7.4), 100 mM NaCl, and 5 mM EDTA in a 10,000 molecular weight cut-off dialysis cassette (Pierce). Protein concentration was determined with the BCA assay (Pierce) using bovine serum albumin as a standard. The point variants of GlfT2 were expressed and purified identically to the wild-type protein.

Production of C. diphtheriae UGM—The pET-24a::*glf*-His_6 plasmid was transformed into BL21(DE3) Tuner *E. coli* (Novagen) by electroporation. Cultures were grown in LB medium supplemented with 50 μg/ml kanamycin at 37 °C until A_{600} 0.6. Cells were cooled on ice, and isopropyl-β-D-thiogalactopyranoside was added to 0.1 mM to induce *glf*-His_6 expression. After 18 h at 20 °C, cells were harvested by centrifugation (5000 × *g*), and cell pellets were stored at −80 °C until use. Cells were thawed on ice and resuspended in 50 mM potassium phosphate (pH 7.4), 300 mM NaCl, and 25 mM imidazole (20 ml/liter of growth). Cells were disrupted by lysozyme, Triton X-100 (0.1% v/v), and sonication (Branson Sonifer 450), and phenylmethylsulfonyl fluoride was added to 1 mM. Cellular debris was cleared by centrifugation (22,000 × *g*, 1 h, 4 °C). The lysate was filtered (0.22 mM, Amicon) and applied to a 1-ml HisTrap column (GE Healthcare) at 0.75 ml/min on an AKTA FPLC (Amersham Biosciences). Protein was eluted with a linear gradient of 25–400 mM imidazole in 50 mM potassium phosphate (pH 7.4), 300 mM NaCl. Fractions of >80% pure were combined and dialyzed at 4 °C against 2 liters of 50 mM potassium phosphate (pH 7.0), 300 mM NaCl, and then 2 liters of 50 mM potassium phosphate (pH 7.0), 5 mM NaCl. The dialyzed solution was applied to a 1-ml HiTrap Q HP column (GE Healthcare) on an AKTA FPLC. Purified protein was eluted with a gradient using 50 mM potassium phosphate (pH 7.0), 1 M NaCl. Fractions were analyzed for purity using SDS-PAGE and Coomassie Blue staining. Fractions >95% pure were collected, pooled, and dialyzed against 50 mM potassium phosphate (pH 7.0) and 150 mM NaCl. Typical yields of the two-step purification were 1.5 mg/liter of culture. Protein concentration was determined by absorbance of the flavin cofactor at 450 nm (e_{450} = 11,300 $M^{-1}cm^{-1}$). Samples were stored at 4 °C until use.

Enzymatic Activity of C. diphtheriae UGM—The enzymatic activity of UGM was determined 1 day after purification using an HPLC-based assay (45, 73). Reactions were performed using 20 nM *C. diphtheriae* UGM in 50 mM potassium phosphate (pH 7.0) and 20 mM freshly prepared sodium dithionite in a volume of either 50 μl or 80 μl. Enzyme activity was initiated with the rapid addition of chemically synthesized UDP-α-d-Gal*f* at varying concentrations (72). Reactions were quenched by the addition of an equal volume of a 1:1 (v:v) mixture of chloroform: methanol. The aqueous and organic phases were separated by centrifugation, and the aqueous phase was assayed using a CarboPac PA-100 column (Dionex) on a Waters HPLC. The added substrate, UDP-Gal*f*, and major product, UDP-Gal*p*, were separated via isocratic elution using 200 mM ammonium acetate (pH 8.0) and monitored via absorbance of the uridine at 262 nm. Initial velocities were calculated based on the initial concentration of substrate and integration of the HPLC chromatograph. Steady-state kinetic constants were determined by nonlinear regression analysis with Prism 4 (Graphpad). Quantified error represents the S.D. of triplicate measurements.

Inhibition of C. diphtheriae UGM—Inhibition of UGM was assayed using the HPLC-based assay described above. Typical reactions were performed with 20 nM *C. diphtheriae* UGM, 50 μM UDP-Gal*f*, and 20 mM freshly prepared sodium dithionite in 50 mM potassium phosphate (pH 7.0) and in a final volume of 80 μl. The UDP was dissolved in water and assayed at 15 μM. The 2-aminothiazole-based inhibitors **1**–**3** were dissolved in DMSO (dimethyl sulfoxide) and were all assayed at 15 μM (total concentration of DMSO equaled 1%). DMSO was used as a vehicle control at 1%. The percent of UDP-Gal*f* converted by the enzyme was determined by integration of the chromatograph, and the data were normalized to the activity of a 50 μM UDP-Gal*f* reaction in the absence of inhibitor or solvent vehicle. Each data point was performed in triplicate, and *error bars* represent the S.D. of the mean.

The IC_{50} of **1** was determined using the HPLC-based assay described above. The inhibitor concentration was adjusted, whereas the other components were at a constant concentration of 20 nM *C. diphtheriae* UGM, 50 μM UDP-Gal*f*, and 20 mM freshly prepared sodium dithionite. The percentage of DMSO in all reactions was 1%. The fraction of UDP-Gal*f* converted to UDP-Gal*p* was determined by integration of the HPLC chromatograph. Data were plotted using GraphPad Prism 4 and fit using the one site competition model.

FP to Measure Binding Constants to C. diphtheriae UGM—The affinity of the FP probe for *C. diphtheriae* UGM was determined by varying UGM concentration (17 nM constant probe concentration). Binding was measured in 50 mM potassium phosphate (pH 7.0) using 384-well, black microtiter plates (Corning) with a total volume of 30 μl per well. All points result from assays performed in triplicate, with fluorescence polarization measurements taken on an Infinite M1000 plate reader (Tecan). Data were plotted using GraphPad Prism 4 and fit using the one site competition model. To measure the apparent affinity of the small molecules for *C. diphtheriae* UGM, an assay similar to that described above was employed. Specifically, 17 nM UDP-10C-fluorescein probe, 120 nM *C. diphtheriae* UGM, and varying amounts of inhibitor were assayed in 50 mM potassium phosphate (pH 7.0). Each data point is the result of measurements performed in triplicate; *error bars* represent the S.D. of the mean. Data were plotted using GraphPad Prism 4 and fit with the one site competition model. To determine binding constants, the equation $K_{app} = K_d(1 + ([I]/K_i))$ was used, where $[I]$ = 17 nM and K_i = 25 nM (as determined in this study).

Bioactivity Plate Assay—C. glutamicum ATCC 13032 were obtained from the ATCC. *C. glutamicum* was grown in LB media at 30 °C until A_{600} = 1.5. This culture (400 μl) was used to seed 40 ml of prewarmed LB agar with bacteria. The seeded LB agar was poured into a sterile Omnitray (Nunc), and a sterile 96-well PCR plate was placed on top. After solidification of the agar, the PCR rack was removed to leave a plate with live embedded *C. glutamicum* and shallow wells for direct comparison of small molecule bioactivity. To each well, 10 μl of a solution of kanamycin, AT91, or ED103 were added. Kanamycin, dissolved in water, was assayed in the following concentrations: 500 ng/ml, 1 μg/ml, 10 μg/ml, 50 μg/ml, 100 μg/ml, 500 μg/ml. Compounds **1** and **3**, dissolved in DMSO, were assayed at the following concentrations: 63 μM, 125 μM, 250 μM, 0.5 mM, 1

mM, 2 mM. The plate was incubated at 25 °C for 45 h and imaged using a Fotodyne lightbox and camera. Using this assay, inhibition of growth was observed in the wells where 10 μl of 10 μg/ml (21 μM) kanamycin was added, and 10 μl of 125 μM compound **1** was added. No growth inhibition was observed when using compound **3**.

MALDI Mass Spectrometric Analysis of C. diphtheriae His$_6$-GlfT2 Enzymatic Activity—Reactions were performed in a total volume of 60 μl and contained 0.2 μM His$_6$-*Cdip*GlfT2, 200 μM acceptor substrate, 1 mM UDP-Gal*f*, 50 mM HEPES (pH 7.0), 25 mM magnesium chloride ($MgCl_2$), and 100 mM NaCl. Reactions were typically allowed to proceed for 20 h at 25 °C until they were quenched with the addition of 60 μl of a 1:1 mixture of chloroform:methanol to precipitate protein. Samples were concentrated by evaporation to dryness under vacuum using a SpeedVac SC100 (Varian). Samples were resuspended in 50 μl of 50% acetonitrile in water. Samples were spotted at a 1:3 ratio with α-cyano-4-hydroxycinnamic acid matrix. Spectra were collected using a Bruker Ultraflex III mass spectrometer.

Kinetic Assay of C. diphtheriae His$_6$-GlfT2 Activity—A coupled enzymatic assay that detects UDP release was employed to measure the kinetic activity of His$_6$-*Cdip*GlfT2 (37, 50). Protein activity was measured in a total volume of 120 μl using a 1-cm path length quartz cuvette containing a solution of 50 mM HEPES (pH 7.0), 25 mM $MgCl_2$, 100 mM NaCl, 300 units of pyruvate kinase (Sigma), 20 units of lactate dehydrogenase (Sigma), 250 μM reduced nicotinamide adenine dinucleotide (NADH), 500 μM phosphoenolpyruvate, and 0.2 μM His$_6$-*Cdip*GlfT2. The oxidation of NADH to yield NAD^+ was monitored over time using a Cary 50 Bio UV-visible spectrophotometer (Varian) at 340 nm. Once a steady baseline was observed, UDP-Gal*f* was added to a final concentration of 1.25 mM. Once the baseline again stabilized, acceptor substrate was added to the desired concentration. The rate of UDP-Gal*f* consumption was determined from the negative slope of the linear portion of NADH absorbance using $\epsilon_{340} = 6300\ M^{-1}\ cm^{-1}$.

Author Contributions—M. R. L. and L. L. K. conceived the study. M. R. L. and D. A. W. performed the studies. DAW, M. R. L., and L. L. K. analyzed the data and wrote the manuscript.

Acknowledgments—MALDI-TOF mass spectrometry data were obtained at the University of Wisconsin (UW)-Madison Chemistry Instrument Center Mass Spectrometry Facility on a Bruker Ultraflex III Instrument that was supported by the National Institutes of Health (Center for Research Resources 1S10RR024601).Additional experiments were carried out at the UW-Madison Biophysics Instrumentation Facility, which is supported by UW-Madison, National Science Foundation Grant BIR-9512577 and National Institutes of Health Grant S10 RR13790. We acknowledge R. A. Splain for synthesis of the synthetic acceptor substrates used in this study and M. A. Martinez Farias for synthesis of the FP probes. We thank H. L. Hodges and A. M. Justen for helpful discussion and help preparing the manuscript.

References

1. Dover, L. G., Cerdeño-Tárraga, A. M., Pallen, M. J., Parkhill, J., and Besra, G. S. (2004) Comparative cell wall core biosynthesis in the mycolated pathogens, *Mycobacterium tuberculosis* and *Corynebacterium diphtheriae*. *FEMS Microbiol. Rev.* **28,** 225–250
2. Crick, D. C., Mahapatra, S., and Brennan, P. J. (2001) Biosynthesis of the arabinogalactan-peptidoglycan complex of *Mycobacterium tuberculosis*. *Glycobiology* **11,** 107R–118R
3. Briken, V., Porcelli, S. A., Besra, G. S., and Kremer, L. (2004) Mycobacterial lipoarabinomannan and related lipoglycans: from biogenesis to modulation of the immune response. *Mol. Microbiol.* **53,** 391–403
4. Angala, S. K., Belardinelli, J. M., Huc-Claustre, E., Wheat, W. H., and Jackson, M. (2014) The cell envelope glycoconjugates of *Mycobacterium tuberculosis*. *Crit. Rev. Biochem. Mol. Biol.* **49,** 361–399
5. Daffe, M., Brennan, P. J., and McNeil, M. (1990) Predominant structural features of the cell wall arabinogalactan of *Mycobacterium tuberculosis* as revealed through characterization of oligoglycosyl alditol fragments by gas chromatography/mass spectrometry and by ^1H and ^{13}C NMR analyses. *J. Biol. Chem.* **265,** 6734–6743
6. Besra, G. S., Khoo, K. H., McNeil, M. R., Dell, A., Morris, H. R., and Brennan, P. J. (1995) A new interpretation of the structure of the mycolyl-arabinogalactan complex of *Mycobacterium tuberculosis* as revealed through characterization of oligoglycosylalditol fragments by fast-atom bombardment mass spectrometry and ^1H nuclear magnetic resonance spectroscopy. *Biochemistry* **34,** 4257–4266
7. Puech, V., Chami, M., Lemassu, A., Lanéelle, M. A., Schiffler, B., Gounon, P., Bayan, N., Benz, R., and Daffé, M. (2001) Structure of the cell envelope of corynebacteria: importance of the non-covalently bound lipids in the formation of the cell wall permeability barrier and fracture plane. *Microbiology* **147,** 1365–1382
8. Jankute, M., Grover, S., Birch, H. L., and Besra, G. S. (2014) Genetics of mycobacterial arabinogalactan and lipoarabinomannan assembly. *Microbiol. Spectr.* **2,** MGM2-0013-2013 (10.1128/microbiolspec.MGM2-0013-2013)
9. Kaur, D., Guerin, M. E., Skovierová, H., Brennan, P. J., and Jackson, M. (2009) Chapter 2: Biogenesis of the cell wall and other glycoconjugates of *Mycobacterium tuberculosis*. *Adv. Appl. Microbiol.* **69,** 23–78
10. Bansal-Mutalik, R., and Nikaido, H. (2014) Mycobacterial outer membrane is a lipid bilayer and the inner membrane is unusually rich in diacyl phosphatidylinositol dimannosides. *Proc. Natl. Acad. Sci. U.S.A.* **111,** 4958–4963
11. Zuber, B., Chami, M., Houssin, C., Dubochet, J., Griffiths, G., and Daffé, M. (2008) Direct visualization of the outer membrane of mycobacteria and corynebacteria in their native state. *J. Bacteriol.* **190,** 5672–5680
12. Weston, A., Stern, R. J., Lee, R. E., Nassau, P. M., Monsey, D., Martin, S. L., Scherman, M. S., Besra, G. S., Duncan, K., and McNeil, M. R. (1997) Biosynthetic origin of mycobacterial cell wall galactofuranosyl residues. *Tuber. Lung Dis.* **78,** 123–131
13. Pan, F., Jackson, M., Ma, Y., and McNeil, M. (2001) Cell wall core galactofuran synthesis is essential for growth of mycobacteria. *J. Bacteriol.* **183,** 3991–3998
14. Mikusová, K., Belánová, M., Korduláková, J., Honda, K., McNeil, M. R., Mahapatra, S., Crick, D. C., and Brennan, P. J. (2006) Identification of a novel galactosyltransferase involved in biosynthesis of the mycobacterial cell wall. *J. Bacteriol.* **188,** 6592–6598
15. Martinez Farias, M. A., Kincaid, V. A., Annamalai, V. R., and Kiessling, L. L. (2014) Isoprenoid phosphonophosphates as glycosyltransferase acceptor substrates. *J. Am. Chem. Soc.* **136,** 8492–8495
16. Mikusová, K., Yagi, T., Stern, R., McNeil, M. R., Besra, G. S., Crick, D. C., and Brennan, P. J. (2000) Biosynthesis of the galactan component of the mycobacterial cell wall. *J. Biol. Chem.* **275,** 33890–33897
17. Kremer, L., Dover, L. G., Morehouse, C., Hitchin, P., Everett, M., Morris, H. R., Dell, A., Brennan, P. J., McNeil, M. R., Flaherty, C., Duncan, K., and Besra, G. S. (2001) Galactan biosynthesis in *Mycobacterium tuberculosis*: identification of a bifunctional UDP-galactofuranosyltransferase. *J. Biol. Chem.* **276,** 26430–26440
18. Rose, N. L., Completo, G. C., Lin, S. J., McNeil, M., Palcic, M. M., and Lowary, T. L. (2006) Expression, purification, and characterization of a galactofuranosyltransferase involved in *Mycobacterium tuberculosis* arabinogalactan biosynthesis. *J. Am. Chem. Soc.* **128,** 6721–6729
19. May, J. F., Splain, R. A., Brotschi, C., and Kiessling, L. L. (2009) A tethering mechanism for length control in a processive carbohydrate polymerization. *Proc. Natl. Acad. Sci. U.S.A.* **106,** 11851–11856

20. Alderwick, L. J., Radmacher, E., Seidel, M., Gande, R., Hitchen, P. G., Morris, H. R., Dell, A., Sahm, H., Eggeling, L., and Besra, G. S. (2005) Deletion of Cg-emb in corynebacterianeae leads to a novel truncated cell wall arabinogalactan, whereas inactivation of Cg-ubiA results in an arabinan-deficient mutant with a cell wall galactan core. *J. Biol. Chem.* **280,** 32362–32371
21. Horsburgh, C. R., Jr, Barry, C. E., 3rd, and Lange, C. (2015) Treatment of tuberculosis. *N. Engl. J. Med.* **373,** 2149–2160
22. Krawczyk, J., Kohl, T. A., Goesmann, A., Kalinowski, J., and Baumbach, J. (2009) From *Corynebacterium glutamicum* to *Mycobacterium tuberculosis*: towards transfers of gene regulatory networks and integrated data analyses with MycoRegNet. *Nucleic Acids Res.* **37,** e97
23. Seidel, M., Alderwick, L. J., Sahm, H., Besra, G. S., and Eggeling, L. (2007) Topology and mutational analysis of the single Emb arabinofuranosyltransferase of *Corynebacterium glutamicum* as a model of Emb proteins of *Mycobacterium tuberculosis*. *Glycobiology* **17,** 210–219
24. Portevin, D., De Sousa-D'Auria, C., Houssin, C., Grimaldi, C., Chami, M., Daffé, M., and Guilhot, C. (2004) A polyketide synthase catalyzes the last condensation step of mycolic acid biosynthesis in mycobacteria and related organisms. *Proc. Natl. Acad. Sci. U.S.A.* **101,** 314–319
25. Seidel, M., Alderwick, L. J., Birch, H. L., Sahm, H., Eggeling, L., and Besra, G. S. (2007) Identification of a novel arabinofuranosyltransferase AftB involved in a terminal step of cell wall arabinan biosynthesis in Corynebacterineae, such as *Corynebacterium glutamicum* and *Mycobacterium tuberculosis*. *J. Biol. Chem.* **282,** 14729–14740
26. Sassetti, C. M., Boyd, D. H., and Rubin, E. J. (2003) Genes required for mycobacterial growth defined by high density mutagenesis. *Mol. Microbiol.* **48,** 77–84
27. Alderwick, L. J., Seidel, M., Sahm, H., Besra, G. S., and Eggeling, L. (2006) Identification of a novel arabinofuranosyltransferase (AftA) involved in cell wall arabinan biosynthesis in *Mycobacterium tuberculosis*. *J. Biol. Chem.* **281,** 15653–15661
28. Jankute, M., Cox, J. A., Harrison, J., and Besra, G. S. (2015) Assembly of the mycobacterial cell wall. *Annu. Rev. Microbiol.* **69,** 405–423
29. Telenti, A., Philipp, W. J., Sreevatsan, S., Bernasconi, C., Stockbauer, K. E., Wieles, B., Musser, J. M., and Jacobs, W. R., Jr. (1997) The emb operon, a gene cluster of *Mycobacterium tuberculosis* involved in resistance to ethambutol. *Nat. Med.* **3,** 567–570
30. Goude, R., Amin, A. G., Chatterjee, D., and Parish, T. (2009) The arabinosyltransferase EmbC is inhibited by ethambutol in *Mycobacterium tuberculosis*. *Antimicrob. Agents Chemother.* **53,** 4138–4146
31. Minnikin, D. E. (1982) Lipids: complex lipids, their chemistry, biosynthesis, and roles. In *The Biology of the Mycobacteria* (Ratledge, C., and Stanford, J., eds.) pp. 95–184, Academic Press Inc., New York
32. Birch, H. L., Alderwick, L. J., Rittmann, D., Krumbach, K., Etterich, H., Grzegorzewicz, A., McNeil, M. R., Eggeling, L., and Besra, G. S. (2009) Identification of a terminal rhamnopyranosyltransferase (RptA) involved in *Corynebacterium glutamicum* cell wall biosynthesis. *J. Bacteriol.* **191,** 4879–4887
33. Szczepina, M. G., Zheng, R. B., Completo, G. C., Lowary, T. L., and Pinto, B. M. (2009) STD-NMR studies suggest that two acceptor substrates for GlfT2, a bifunctional galactofuranosyltransferase required for the biosynthesis of *Mycobacterium tuberculosis* arabinogalactan, compete for the same binding site. *Chembiochem* **10,** 2052–2059
34. Brown, C. D., Rusek, M. S., and Kiessling, L. L. (2012) Fluorosugar chain termination agents as probes of the sequence specificity of a carbohydrate polymerase. *J. Am. Chem. Soc.* **134,** 6552–6555
35. Peltier, P., Beláňová, M., Dianišková, P., Zhou, R., Zheng, R. B., Pearcey, J. A., Joe, M., Brennan, P. J., Nugier-Chauvin, C., Ferrières, V., Lowary, T. L., Daniellou, R., and Mikušová, K. (2010) Synthetic UDP-furanoses as potent inhibitors of mycobacterial galactan biogenesis. *Chem. Biol.* **17,** 1356–1366
36. May, J. F., Levengood, M. R., Splain, R. A., Brown, C. D., and Kiessling, L. L. (2012) A processive carbohydrate polymerase that mediates bifunctional catalysis using a single active site. *Biochemistry* **51,** 1148–1159
37. Levengood, M. R., Splain, R. A., and Kiessling, L. L. (2011) Monitoring processivity and length control of a carbohydrate polymerase. *J. Am. Chem. Soc.* **133,** 12758–12766
38. Yamatsugu, K., Splain, R. A., and Kiessling, L. L. (2016) Fidelity and promiscuity of a mycobacterial glycosyltransferase. *J. Am. Chem. Soc.* **138,** 9205–9211
39. Wheatley, R. W., Zheng, R. B., Richards, M. R., Lowary, T. L., and Ng, K. K. (2012) Tetrameric structure of the GlfT2 galactofuranosyltransferase reveals a scaffold for the assembly of mycobacterial arabinogalactan. *J. Biol. Chem.* **287,** 28132–28143
40. Bastin, D. A., Stevenson, G., Brown, P. K., Haase, A., and Reeves, P. R. (1993) Repeat unit polysaccharides of bacteria: a model for polymerization resembling that of ribosomes and fatty acid synthetase, with a novel mechanism for determining chain length. *Mol. Microbiol.* **7,** 725–734
41. Woodward, R., Yi, W., Li, L., Zhao, G., Eguchi, H., Sridhar, P. R., Guo, H., Song, J. K., Motari, E., Cai, L., Kelleher, P., Liu, X., Han, W., Zhang, W., Ding, Y., Li, M., and Wang, P. G. (2010) In vitro bacterial polysaccharide biosynthesis: defining the functions of Wzy and Wzz. *Nat. Chem. Biol.* **6,** 418–423
42. Hagelueken, G., Clarke, B. R., Huang, H., Tuukkanen, A., Danciu, I., Svergun, D. I., Hussain, R., Liu, H., Whitfield, C., and Naismith, J. H. (2015) A coiled-coil domain acts as a molecular ruler to regulate O-antigen chain length in lipopolysaccharide. *Nat. Struct. Mol. Biol.* **22,** 50–56
43. Dykhuizen, E. C., May, J. F., Tongpenyai, A., and Kiessling, L. L. (2008) Inhibitors of UDP-galactopyranose mutase thwart mycobacterial growth. *J. Am. Chem. Soc.* **130,** 6706–6707
44. Kincaid, V. A., London, N., Wangkanont, K., Wesener, D. A., Marcus, S. A., Héroux, A., Nedyalkova, L., Talaat, A. M., Forest, K. T., Shoichet, B. K., and Kiessling, L. L. (2015) Virtual screening for UDP-galactopyranose mutase ligands identifies a new class of antimycobacterial agents. *ACS Chem. Biol.* **10,** 2209–2218
45. Lee, R., Monsey, D., Weston, A., Duncan, K., Rithner, C., and McNeil, M. (1996) Enzymatic synthesis of UDP-galactofuranose and an assay for UDP-galactopyranose mutase based on high-performance liquid chromatography. *Anal. Biochem.* **242,** 1–7
46. Zhang, Q., and Liu, H. (2000) Studies of UDP-galactopyranose mutase from *Escherichia coli*: an unusual role of reduced FAD in its catalysis. *J. Am. Chem. Soc.* **122,** 9065–9070 (10.1021/ja001333z)
47. Chad, J. M., Sarathy, K. P., Gruber, T. D., Addala, E., Kiessling, L. L., and Sanders, D. A. (2007) Site-directed mutagenesis of UDP-galactopyranose mutase reveals a critical role for the active-site, conserved arginine residues. *Biochemistry* **46,** 6723–6732
48. Dykhuizen, E. C., and Kiessling, L. L. (2009) Potent ligands for prokaryotic UDP-galactopyranose mutase that exploit an enzyme subsite. *Org. Lett.* **11,** 193–196
49. Soltero-Higgin, M., Carlson, E. E., Phillips, J. H., and Kiessling, L. L. (2004) Identification of inhibitors for UDP-galactopyranose mutase. *J. Am. Chem. Soc.* **126,** 10532–10533
50. Rose, N. L., Zheng, R. B., Pearcey, J., Zhou, R., Completo, G. C., and Lowary, T. L. (2008) Development of a coupled spectrophotometric assay for GlfT2, a bifunctional mycobacterial galactofuranosyltransferase. *Carbohydr. Res.* **343,** 2130–2139
51. Coyle, M. B., and Lipsky, B. A. (1990) Coryneform bacteria in infectious diseases: clinical and laboratory aspects. *Clin. Microbiol. Rev.* **3,** 227–246
52. Funke, G., von Graevenitz, A., Clarridge, J. E., 3rd, and Bernard, K. A. (1997) Clinical microbiology of coryneform bacteria. *Clin. Microbiol. Rev.* **10,** 125–159
53. Hermann, T. (2003) Industrial production of amino acids by coryneform bacteria. *J. Biotechnol.* **104,** 155–172
54. Daffe, M., McNeil, M., and Brennan, P. J. (1993) Major structural features of the cell wall arabinogalactans of *Mycobacterium*, *Rhodococcus*, and *Nocardia* spp. *Carbohydr. Res.* **249,** 383–398
55. Kacem, R., De Sousa-D'Auria, C., Tropis, M., Chami, M., Gounon, P., Leblon, G., Houssin, C., and Daffé, M. (2004) Importance of mycoloyltransferases on the physiology of *Corynebacterium glutamicum*. *Microbiology* **150,** 73–84
56. Beverley, S. M., Owens, K. L., Showalter, M., Griffith, C. L., Doering, T. L., Jones, V. C., and McNeil, M. R. (2005) Eukaryotic UDP-galactopyranose mutase (GLF gene) in microbial and metazoal pathogens. *Eukaryot. Cell* **4,** 1147–1154

57. Wesener, D. A., May, J. F., Huffman, E. M., and Kiessling, L. L. (2013) UDP-galactopyranose mutase in nematodes. *Biochemistry* **52,** 4391–4398
58. Soltero-Higgin, M., Carlson, E. E., Gruber, T. D., and Kiessling, L. L. (2004) A unique catalytic mechanism for UDP-galactopyranose mutase. *Nat. Struct. Mol. Biol.* **11,** 539–543
59. Wang, T. S., Manning, S. A., Walker, S., and Kahne, D. (2008) Isolated peptidoglycan glycosyltransferases from different organisms produce different glycan chain lengths. *J. Am. Chem. Soc.* **130,** 14068–14069
60. Glauner, B. (1988) Separation and quantification of muropeptides with high-performance liquid chromatography. *Anal. Biochem.* **172,** 451–464
61. Raetz, C. R., and Whitfield, C. (2002) Lipopolysaccharide endotoxins. *Annu. Rev. Biochem.* **71,** 635–700
62. Yother, J. (2011) Capsules of *Streptococcus pneumoniae* and other bacteria: paradigms for polysaccharide biosynthesis and regulation. *Annu. Rev. Microbiol.* **65,** 563–581
63. Gründling, A., and Schneewind, O. (2007) Synthesis of glycerol phosphate lipoteichoic acid in *Staphylococcus aureus*. *Proc. Natl. Acad. Sci. U.S.A.* **104,** 8478–8483
64. Paulsen, I. T., Beness, A. M., and Saier, M. H. (1997) Computer-based analyses of the protein constituents of transport systems catalyzing export of complex carbohydrates in bacteria. *Microbiology* **143,** 2685–2699
65. Tocilj, A., Munger, C., Proteau, A., Morona, R., Purins, L., Ajamian, E., Wagner, J., Papadopoulos, M., Van Den Bosch, L., Rubinstein, J. L., Féthière, J., Matte, A., and Cygler, M. (2008) Bacterial polysaccharide co-polymerases share a common framework for control of polymer length. *Nat. Struct. Mol. Biol.* **15,** 130–138
66. Lerouge, I., and Vanderleyden, J. (2002) O-antigen structural variation: mechanisms and possible roles in animal/plant-microbe interactions. *FEMS Microbiol. Rev.* **26,** 17–47
67. Cantarel, B. L., Coutinho, P. M., Rancurel, C., Bernard, T., Lombard, V., and Henrissat, B. (2009) The carbohydrate-active EnZymes database (CAZy): an expert resource for glycogenomics. *Nucleic Acids Res.* **37,** D233–D238
68. Somerville, C. (2006) Cellulose synthesis in higher plants. *Annu. Rev. Cell Dev. Biol.* **22,** 53–78
69. Ventura, C. L., Cartee, R. T., Forsee, W. T., and Yother, J. (2006) Control of capsular polysaccharide chain length by UDP-sugar substrate concentrations in *Streptococcus pneumoniae*. *Mol. Microbiol.* **61,** 723–733
70. Forsee, W. T., Cartee, R. T., and Yother, J. (2009) A kinetic model for chain length modulation of *Streptococcus pneumoniae* cellubiuronan capsular polysaccharide by nucleotide sugar donor concentrations. *J. Biol. Chem.* **284,** 11836–11844
71. Berg, S., Starbuck, J., Torrelles, J. B., Vissa, V. D., Crick, D. C., Chatterjee, D., and Brennan, P. J. (2005) Roles of conserved proline and glycosyltransferase motifs of EmbC in biosynthesis of lipoarabinomannan. *J. Biol. Chem.* **280,** 5651–5663
72. Marlow, A. L., and Kiessling, L. L. (2001) Improved chemical synthesis of UDP-galactofuranose. *Org. Lett.* **3,** 2517–2519
73. Partha, S. K., Sadeghi-Khomami, A., Slowski, K., Kotake, T., Thomas, N. R., Jakeman, D. L., and Sanders, D. A. (2010) Chemoenzymatic synthesis, inhibition studies, and X-ray crystallographic analysis of the phosphono analog of UDP-Galp as an inhibitor and mechanistic probe for UDP-galactopyranose mutase. *J. Mol. Biol.* **403,** 578–590

Comparing Galactan Biosynthesis in *Mycobacterium tuberculosis* and *Corynebacterium diphtheriae*

Darryl A. Wesener, Matthew R. Levengood and Laura L. Kiessling

J. Biol. Chem. 2017, 292:2944-2955.
doi: 10.1074/jbc.M116.759340 originally published online December 30, 2016